

# Experimental study of moment redistribution and load carrying capacity of externally prestressed continuous composite beams

Shiming Chen<sup>†</sup>, Yuanlin Jia<sup>‡</sup> and Xindi Wang<sup>‡†</sup>

*School of Civil Engineering, Tongji University, Shanghai, China*

*(Received July 7, 2008, Accepted March 3, 2009)*

**Abstract.** A comparative experimental study of prestressed continuous steel-concrete composite beams was carried out. Two continuous composite beams were tested, one of which was plain continuous steel-concrete composite beam, while the other was a composite beam prestressed with external tendons. Cracking behavior and the load carrying capacity of the beams were investigated experimentally. Full plasticity was developed in the mid-span section each beam, the maximum moments attained at the internal support sections however were governed by local buckling which was related to the slenderness of composite section. It was found that in hogging moment regions, the ultimate resistance of an externally prestressed composite beam would be governed by either distortional lateral buckling or local buckling, or interactive mode of these two buckling patterns. The results show that exerting prestressing on a continuous composite beam with external tendons will increase the extent of internal force and moment redistribution in the beam. The influences of local and distortional buckling on the behaviors of the composite continuous beams are discussed. The Moment redistribution and the load carrying capacity of the prestressed continuous composite beams are evaluated, and it is found that at the ultimate state, the moment redistribution in the prestressed continuous composite beams is greater than that in non-prestressed composite beams.

**Keywords:** continuous composite beam; prestressed; external tendon; moment redistribution.

---

## 1. Introduction

Composite steel-concrete beams prestressed with high strength external tendons are known for many advantages as compared with non-prestressed composite beams. Both simple and continuous beams can be prestressed and the external prestressing tendons may be rectilinear or draped with a path fixed by end anchorages and by intermediate saddle points in order to induce a set of forces on the beams which opposes the external loads. Adding prestressing along the steel bottom flange composite beam under positive moment will make the beam less deflected and increase the ultimate capacity; while adding prestressing in hogging moment region can eliminate cracks in the concrete slab due to the negative bending.

---

<sup>†</sup> Professor, Corresponding author, E-mail: [chensm@mail.tongji.edu.cn](mailto:chensm@mail.tongji.edu.cn)

<sup>‡</sup> Ph.D. Candidate, E-mail: [jiayuanlin2003@yahoo.com.cn](mailto:jiayuanlin2003@yahoo.com.cn)

<sup>‡†</sup> Ph.D. Candidate, E-mail: [compositebeam@yahoo.com.cn](mailto:compositebeam@yahoo.com.cn)

Behavior and failure mechanism of the prestressed composite beams with external tendons were investigated by Saadatmanesh, Ayyub and Sohn (1989, 1990, 1992), Uy and Craine (2004), Chen and Gu (2005), Chen (2005) and Lorenc and Kubica (2006). Slip effect on behavior of the externally prestressed composite beams was also investigated by Nie (2007) experimentally and analytically. However, the most beams studied were simply supported either in positive or in negative bending. Limited experimental investigations on the prestressed composite continuous beams were reported in literatures. An experimental investigation on the external prestressed steel-concrete composite continuous beams was reported by Zong *et al.* (2002), in which one conventional non-prestressed and five prestressed two-span composite continuous beams were tested. It is found that failures of the prestressed composite continuous beams were governed either in crush of the concrete slab at mid-span sections, or in local and distortional buckles at the internal support section. Full plasticity was developed both at the mid-span and at the internal cross sections for all the beams, and substantial moment redistribution was observed for the beams.

Dall'Asta and Zona (2005) proposed a finite element model and conducted a nonlinear analysis on continuous composite beams prestressed by external slipping cables. The effectiveness of the numerical procedure in describing the structural behavior up to the failure has been validated by comparisons with experimental tests available. The validations of the model and findings were later discussed by Chen (2006) on available rotation capacity and moment redistribution of the beams studied. The analytical approach was more recently summarized by Zona *et al.* (2008) and, a simplified method for the analysis of externally prestressed steel-concrete composite beams was proposed. Meanwhile, the effective width of concrete flange in externally prestressed composite beams was also investigated by Chen and Zhang (2006) based on the finite element analysis. Xue *et al.* (2008) presented an experimental program to investigate the long-term behavior of externally prestressed composite beams at the service loads, as affected by time effects, such as creep and shrinkage of concrete slabs and relaxation of prestressing tendons.

The factors that influence behavior and load carrying capacity of prestressed continuous composite beams with external tendons are complex. An important feature of the prestressed composite beams is that under variable loadings, incremental stress will develop in the tendons, which has the secondary bending action on the beam section. In elastic range, the incremental tendon stress could be derived by energy method with compatibility between the beam and the tendons. However, at the ultimate state, the increment stress would be substantial when large deflection occurs in the composite beam. For a continuous composite beam, restrained by the stiff concrete slab on the steel top flange, the steel component in the negative moment region would be prone to buckling which govern the ultimate failure of the beam. The modes of buckling in a continuous beam in negative bending may be local or overall. Overall buckling is now more frequently termed as distortional buckle since the bottom flange, which is in compression and restricted only by the stiffness of the web, buckles sideways and twists. Moreover, in negative bending, exerting prestressing force to the composite beam will increase the axial compressive force in the beam which would lead to a high compression depth in the steel web, make the beam vulnerable to buckling, and reduce the moment rotation capacity of the cross-section.

Local buckling of a composite beam in negative bending is closely link to the width/thickness ratio of the steel compression flange and the depth/thickness ratio of the steel web of the steel beam. In design practice, classification of cross-sections is generally used to identify the stress level attained and stress distribution over the cross-section when local buckling initiates. For instance, full yield can develop through the cross-section before local buckling occurs, if the slenderness is small

or the cross-section is compact, whereas for a non-compact section, or when the slenderness is large, local buckling initiates before yielding occurs in the beam. In EUROCODE 4, composite beams are classified as plastic sections (Class 1), compact sections (Class 2), non-compact sections (Class 3) and slender sections (Class 4). In free of lateral buckling, for a beam with a plastic/or compact section, negative bending moment can reach to the plastic moment if the steel section is fully plastic, and for the non compact section, negative bending moment would be limited to the yield moment, at which the compression steel flange initiates yield.

Moment redistribution based on the global elastic analysis is now widely accepted in design practice for the ultimate limit state design of continuous composite beams. For design purposes, it is essential to assess the moment redistribution capable of in the externally prestressed continuous composite beams. In this study, two two-span continuous composite steel-concrete beams were tested, one of which was a conventional non-prestressed continuous composite beam, and the other was a continuous composite beam prestressed with external tendons. The objective of the experimental program was to study mechanical behavior, failure modes, moment redistribution and prestressing effects of the composite continuous beams prestressed with external tendons both in positive and negative moment regions. The influences of local and distortional buckling on behavior of the beams were discussed and the load carrying capacity of prestressed composite continuous beams was evaluated based on the moment redistribution approach.

## 2. Experimental program

### 2.1 Test specimens

Two full-scale two-span continuous composite beams were erected. Specimen PCCB1 is a continuous composite beam prestressed with external tendons and specimen CCB1 is a conventional non-prestressed continuous composite beam. The geometrical configurations and cross-sections of the two specimens are identical except that no external tendons are provided to beam CCB1. An elevation and cross-sections of specimen PCCB1 are given in Fig. 1. The steel beams used are welded steel plate girders which were manufactured in a steel workshop. The steel top flanges are 120×10 mm and the bottom flanges are 120×14 mm and the steel webs are 255×6 mm. Each span of the beams is 4800 mm, with a 150 mm extent portion overhanging each edge support and the total length of the beams was 9900 mm. The measured dimensions of the specimens are given in Table 1.

A casting in situ concrete slab 550 mm by 9900 mm and 90 mm thick was compositely connected to the steel top flange by shear stud connectors for each beam. Two rows of 16 mm diameter by 65 mm long shear studs were welded to the top flange, with a transverse spacing 76 mm symmetric to the center line of the top flange and a longitudinal spacing of 150 mm. Full shear connection was provided in accordance with Eurocode 4.

The concrete slab in the negative moment regions near the internal support section was reinforced longitudinally with two layers of  $\Phi 16$  (16 mm in diameter) deformed bars, with 30 mm concrete cover top and bottom. The areas of steel rebar over the negative moment regions denoted as  $A_r$  are illustrated in Table 1, where subscripts 'top' and 'bot' refer to the top and bottom layers of the bars. The rest part of the concrete slab which was in positive bending was reinforced with  $\phi 8$  deformed bars (8mm in diameter) in two orthogonal directions.

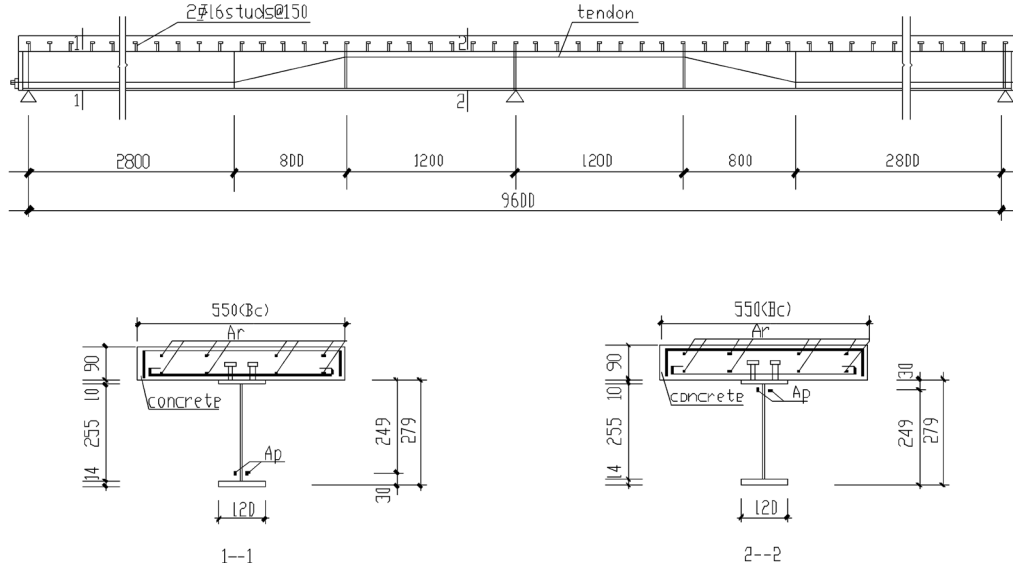


Fig. 1 Elevation and cross-sections of specimen PCCB1 (nominal dimensions)

Table 1 Measured dimensions of the specimens

Specimen	$b_{top}$ mm	$t_{top}$ mm	$d_w$ mm	$t_w$ mm	$b_{bot}$ mm	$t_{bot}$ mm	$A_{r,top}$ mm <sup>2</sup>	$A_{r,bot}$ mm <sup>2</sup>	$A_{p,2}$ mm <sup>2</sup>
CCB1	118.4	9.9	253.5	6	122.8	13.9	803.8	803.8	0
PCCB1	118.4	9.9	253.0	6	121.0	14.0	803.8	803.8	274.8

Table 2 Mechanical properties of materials (N/mm<sup>2</sup>)

	Concrete	Steel Beam					
		Top flange	Bottom flange	Web	Steel rebar	Strands	
$f_{cu}$	34.0	$f_y$	372.3	369.3	372.3	338.4	1680
$f_t$	2.4	$f_u$	552.7	543.3	529.3	510.0	—
$E_c$	$3.15 \times 10^4$	$E_s$	$2.0 \times 10^5$	$2.0 \times 10^5$	$2.0 \times 10^5$	$2.0 \times 10^5$	$1.95.0 \times 10^5$

Bearing stiffeners were welded to the steel web of the beams at each support section.

The measured mean compressive strengths of three cubes at 30 days after casting of the concrete are given in Table 2. The specified characteristic tensile strengths of concrete are used in prediction of the cracking resistance of the specimens. The mean tensile properties of steel for web and flange obtained from tensile coupons test are also summarized in Table 2. The elongation of the steel was 24 (for web) and 28 (for flanges).

The slenderness is 3.8 in the compression flanges and 41.2 in the steel web for all the beams, excluded 4 mm in welding foot. The two beams are in class 3 in accordance with Eurocode 4.

Specimen PCCB1 was designed with two 7 $\phi$ 5 high strength strands, each having a nominal cross

section of  $137.4 \text{ mm}^2$ . The prestressing strands were anchored at the two end plates (25 mm thick) of the beam, 30 mm above the bottom flange and were draped rectilinearly with a path fixed by intermediate points (section 1-1, Fig. 1) and 30 mm below the top steel flange in negative moment regions near the internal support (section 2-2, Fig. 1), each side of steel web, extended along full length of the beam. Post-prestressing was performed with average initial prestressing force of 121 kN each strand (52% of yielding strength of the strands) before the test.

### 2.2 Instrumentations

Each specimen was instrumented with three strain gauges on the web and one strain gauge in the bottom flange at middle span sections. Three strain gauges on the web and two pairs strain gauges on the bottom flange were also mounted in the two cross-sections 100 mm distant from the internal support. The strain gauges on the bottom flanges were installed in pair denoted as west-1, west-2, east-1 and east-2 in such a way that mean compression strains and in-plane bending strains (as a result of possible lateral buckling at high loads) could be picked up as shown in Fig. 2.

Strain gauges were also mounted on the reinforced bars embedded in concrete slab. The deflections were measured by displacement transducers (LVDT) located underneath the bottom flange at mid-span, and 1/4 span each side of the beams. Another two displacement transducers were used to detect the longitudinal slips between the steel beam and the concrete slab at the ends of the beams. Two LVDTs were mounted horizontally to measure the end rotation of the beams. Underneath the east end support of each beam, four load cells were mounted in a group to measure the reaction force of the support.

Instrumentations on specimens PCCB1 and CCB1 are similar except that in specimen PCCB1, each external tendon was instrumented with three strain gauges as illustrate in Fig. 2.

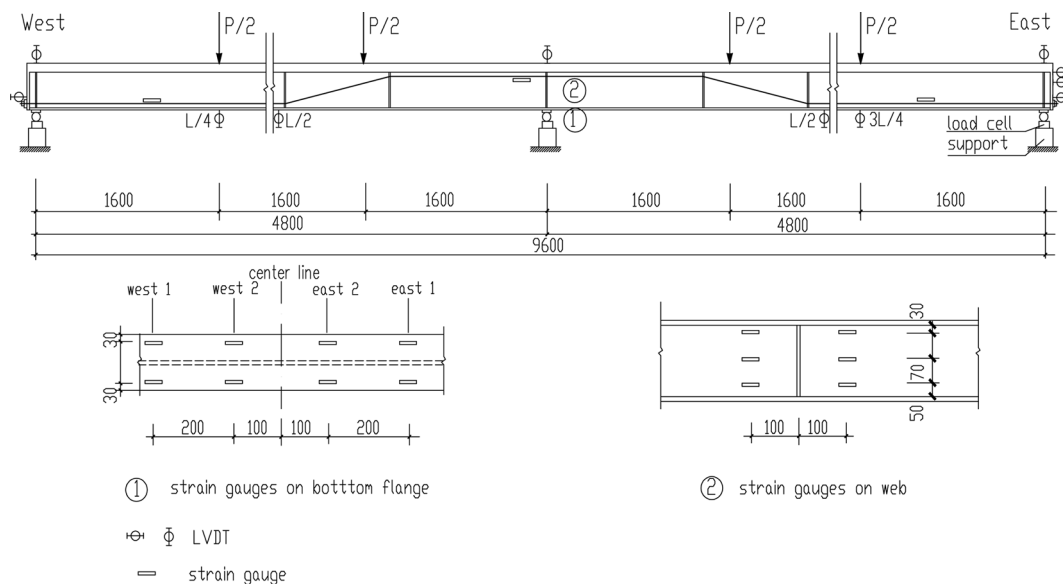


Fig. 2 Loading and instrumentation arrangements



Fig. 3 Test rigs

### *2.3 Testing rigs*

The test rigs are shown in Fig. 3. The load was exerted to the test specimens with two hydraulic Jacks via loading beams each span. The two hydraulic Jacks were connected to one electric-hydraulic driving pump, so that the loading exerted on each span were controlled simultaneously the same. All electric digital data were collected using a Jinjiang 3818 data logger, controlled by a PC computer.

### *2.4 Prestressing on specimen PCCB1*

Post prestressing was exerted on specimen PCCB1 before the loading test. The two strands each side of the steel beam were prestressed alternately to maintain laterally balancing in the beam during the prestressing process. Three strain gauges on each strand were positioned, among which, two in the horizontal segments near the ends of the beam, and one in the horizontal segment near the support section (shown in Fig. 2). The strains measured were calibrated against the exerted prestressing force, so that increase of the prestressing force in the later static load test was able to be detected.

### *2.5 Test procedure and results*

Specimen CCB1: The beam was loaded monotonically. The first crack appeared transversely across at the top of the concrete slab at the internal support section when the applied load each span was 30.7 kN, and subsequent cracks were observed immediately adjacent to the first crack each side of the internal support and spacing of the cracks was between 150 to 200 mm. The outward distortion in the web and lateral buckle in the bottom flanges immediate to the internal support were founded, and in-plane bending induced by lateral buckling was picked in the compression bottom flange near the internal support when the load reached to 278.9 kN. Local buckling was observed in the steel web and an abrupt increase of in-plane strain was also detected in the steel bottom flange when the load reached to 392 kN. The maximum load exerted each span of the beam is 557 kN when one mid-span concrete slab crushed (Fig. 4) and significant buckle in web and in compression flange near the internal support was observed (Fig. 5). After the beam was unloaded, there was a portion of residual web distortion and out plane bending strain in the compression flanges each side



Fig. 4 Concrete crush at mid-span: CCB1



Fig. 5 Local buckling in web and bottom flange: CCB1



Fig. 6 Buckling in web and bottom flange: PCCB1

of the internal support.

Specimen PCCB1: As prestressing was exerted on the specimen before the loading test, there was an upward deflection in each span of the beam. Similar crack patterns were also observed at the top of the concrete slab near the internal support, however a higher load of 95 kN was found for the first crack as compared with specimen CCB1. Lateral buckling was picked in the compression bottom flange near the internal support when the load reached to 253.4 kN, and local buckling in the web was found when the load was 345 kN. The maximum load reached in the test was 618.5 kN, and the beam failed in concrete crush at mid-span and significant in-plane bending in the compression flange were also observed (Fig. 6). After the beam was unloaded, there was residual out plane bending strain in the compression flanges near the internal support.

Load-deflection curves: Fig. 7 are curves of load against mid-span deflection each span for CCB1 and PCCB1. Both beams behaved quite linearly in the load-deflection curves before yielding in the steel bottom flanges at the internal supports, although nonlinearity induced by cracking in concrete slabs near the internal support section already occurred in the previous load levels. The initial upward deflection had contributed to the less deflection in the prestressed beam, and the tangents of the curves of PCCB1 are slightly greater than those of the non-prestressed beam. However before

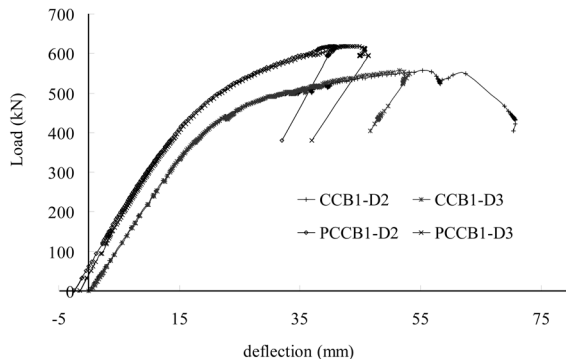


Fig. 7 Load-deflection curves for CCB1 and PCCB1

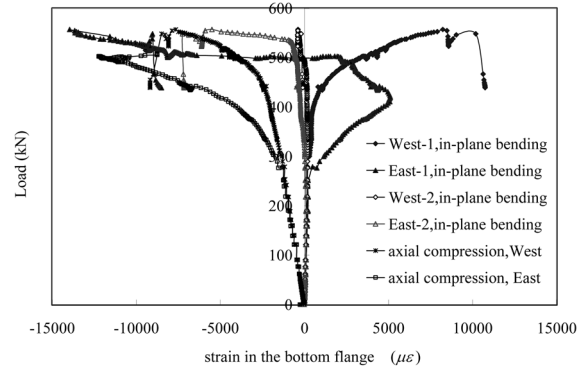


Fig. 8 Strains at steel bottom flange near the internal support (CCB1)

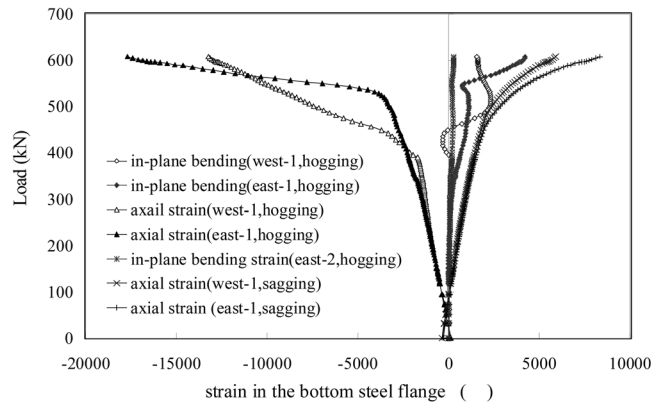


Fig. 9 Strains at steel bottom flange of PCCB1

yielding of the steel beams, they appear quite the same. The reason should be that incremental prestress in the tendons, which is small and develops linearly with the exerted load before the yielding of the steel beam in specimen PCCB1, but increases much faster afterward.

The cracking load denoted as the first crack appearing on the top of the concrete slab and the maximum load of the prestressed beam (PCCB1) are all greater than those of the non-prestressed beam (CCB1). The yielding load at which the steel bottom flange yields near the internal support is 345 kN for specimen PCCB1, being slightly lower than that of specimen CCB1. These characteristic load values and the corresponding moments of the beams are given in Table 3.

**Strain of the steel bars in hogging region:** The strains of steel rebar in negative moment region were measured for both PCCB1 and CCB1. Yielding of the steel rebar at the internal support section occurred at a load of 333.1 kN for CCB1, and 408.5 kN for PCCB1. Then rebar strains developed substantially afterward for both beams.

**Strains of the steel bottom flange in negative moment region:** In-plane strains indicating lateral deformation in the steel bottom flange were picked by a pair of parallel strain gauges. The in-plane bending strains and axial compression strain of the bottom flanges at the cross-sections (shown in Fig. 2) near the internal support varying with the applied load for specimen CCB1 are illustrated in Fig. 8.

Table 3 Load measured at different states for CCB1 and PCCB1

Description	CCB1			PCCB1		
	$P$ kN	$M_h$ kNm	$M_s$ kNm	$P$ kN	$M_h$ kNm	$M_s$ kNm
Concrete cracking	30.7	16.7		95.0	43.8	
Lateral buckle	278.9	141.4	175.9	253.4	138.5	128.4
Internal support bottom flange yield	347.0	174.5	191.1	345.0	167.9	191.8
Local buckle	392.3	189.3	250.7	395.9	187.3	223.1
Maximum Load	557.2	203.0	344.2	618.5	174.2	407.7

Note: subscript  $h$  means hogging internal support, and  $s$  means sagging mid-span.

The in-plane bending strains and the axial strains of the steel bottom flanges at the cross-sections (shown in Fig. 2) close to the internal support and at the mid-span sections of specimen PCCB1 are drawn against applied load and illustrated in Fig. 9. Both beams initiated distortional lateral buckle before yielding in the bottom flange near the internal support, and local buckling in the web and bottom flanges were observed soon after yielding in the bottom flange. The values of the corresponding loads are listed in Table 3. The maximum hogging moment reached at the internal support is 207.7 kNm for specimen CCB1 and is 208.0 kNm for PCCB1.

Prestress increment of the external tendons of PCCB1: Fig. 10 illustrates the prestressing forces in different segments of the external tendons varying with the applied load. The differences in segments of the tendons indicated loss of the prestressing forces which was caused by friction at the intermediate draped points. The prestress increment appeared linearly before the onset of yielding in the beam and then developed faster afterward. The mean initial prestressing forces measured at east, middle and west segments of the two tendons are 100.5 kN, 121.6 kN and 125.2 kN respectively, nevertheless, at the ultimate failure, the tendon forces measured at the east, middle and west segments increased up to 155.5 kN, 164.4 kN and 171.6 kN with the corresponding force increments of 55 kN, 42.8 kN and 46.4 kN respectively.

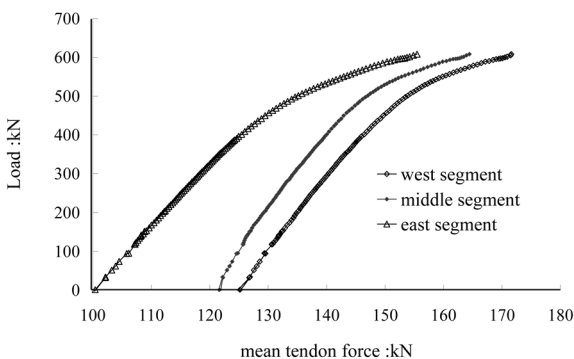


Fig. 10 Tendon forces varying with the applied load

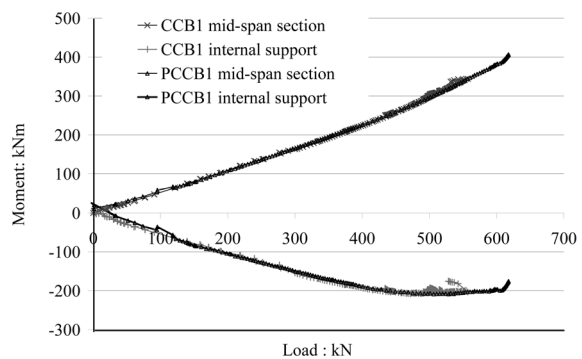


Fig. 11 Moments varying with the applied load

**Moment redistribution:** Fig. 11 illustrates the moments at the mid-span and at the internal support sections varying with the applied load for beam CCB1 and beam PCCB1. The moments are derived based on the whole beam equilibrium from the measured reaction force and the exerted load. The maximum moments at the internal support for the two beams are almost the same, and it appears that the hogging moment developed at that section is restricted by local buckling. Full plasticity was developed in the mid-span sections in the both beams, however specimen PCCB1 sustained a higher sagging moment than that of specimen CCB1 in the mid-span. More moment appears to redistribute from the hogging region to the mid-span sagging regions in the prestressed beam than that appears in the non- prestressed beam.

**Slip measurement** The slips at the two ends of either CCB1 or PCCB1 are less than 0.3 mm. The maximum slips may occur in the middle span, but they were not gauged in the tests. As the beams are designed in full shear connection, influence of shear slip on the performance of the beams should be negligible.

### 3. Discussions

#### 3.1 Classification of cross-section and distortional buckling

Cross-sections of the two beams are identical. The slenderness is 3.8 in the compression flanges and 41.2 in the steel web for all the beams, excluded 4 mm in welding foot, so that the beams are in class 3 cross-section in accordance with Eurocode 4.

Local buckling in the steel web and in the bottom flanges occurred in both CCB1 and PCCB1 after yielding near the internal support section. Distortional lateral buckling was also observed before yielding in the bottom flanges near the internal supports for the two beams. However, both beams were capable of further substantial loading after the onset of lateral buckle. It is likely that lateral buckling in distortional mode will reduce the hogging moment resistance of a composite beam. However it does not certainly represent the ultimate failure of a continuous composite beam whether it is prestressed or non-prestressed, and the maximum hogging moment is governed by local buckling, which is related to the slenderness of cross-section.

#### 3.2 Moment resistance of prestressed composite beams

Fig. 12 illustrates the strain distribution measured over steel sections at the mid-span and at the

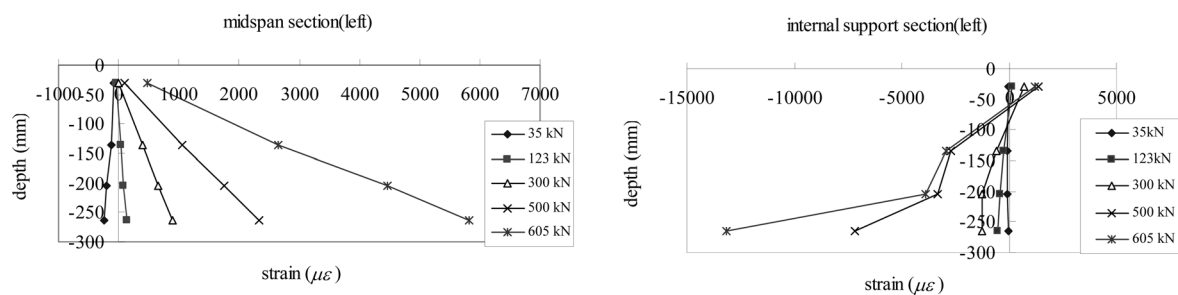


Fig. 12 Strain distribution over the sections at the mid-span and at the internal support: PCCB1

internal support under the different load levels for the prestressed beam (PCCB1). The strain distributed linearly over the steel section at the mid-span section, but there was slight distortion in the steel section near the internal support where the strain did not distribute linear over the depth of the section at the higher load levels since buckling developed in the web and in compression flange.

Nevertheless, to simplify determination of cross-section properties of a prestressed composite beam, however, linear strain distributed over full depth of cross-section is assumed. Cross section properties of the prestressed composite beams are calculated by transforming the concrete section into an equivalent steel section using the modular ratio  $n$  ( $n = E_s/E_c$ , where  $E_s$  is elastic modular of steel and  $E_c$  is elastic modular of concrete). Extreme fibre stress due to the applied load and prestressing force at the top surface of the concrete slab is given by

$$\sigma_c = \frac{M}{nI}y_c + \frac{Te}{nI}y_c - \frac{T}{nA} \quad (1)$$

and the stress at the compression flange of steel beam is given by

$$\sigma_{sf} = \frac{M}{I}y_{bot} + \frac{Te}{I}y_{bot} - \frac{T}{A} \quad (2)$$

where  $M$  = moment due to applied load,  $I$  = moment of inertia of composite section, uncracked transformed section is used before concrete cracking, and cracked transformed section neglecting concrete portion but including steel reinforcement is used after concrete cracking;  $y_c$  and  $y_{bot}$  = distance from the centroid to the extreme fibre of the concrete slab and the compression steel flange respectively;  $A$  = transformed area of the uncracked composite section,  $T$  is the prestressing force, and  $e$  = eccentricity of tendon from centroid of the composite section. Introducing prestressing force  $T$ , moment resistances of the cross-section of a prestressed composite beam can be also derived.

For an externally prestressed composite beam, incremental forces in the tendon would develop and the magnitude of the increments at the ultimate state of the beam varies depending on the geometry and eccentricity as well as the moment regions (positive or negative) of the composite section. In a continuous beam, loss of the prestressing forces caused by friction at the intermediate draped points and relaxation of prestressing tendons will lead to redistribution of incremental tendon forces between different segments of the tendons over the sagging and hogging moment regions of the beam. After cracking in concrete, the tensile force in the concrete flange is shedding to the longitudinal steel reinforcement. For composite beams in negative bending, there are also yield moments at which the steel reinforcing bars yield, but they do not govern the strength of beams in the tests.

At the ultimate state, moment resistance of the prestressed composite section is simplified as the follows

Positive bending: 
$$M_{p,p} = M_p \pm Te_p \quad (3)$$

Negative bending: 
$$M'_{p,p} = M'_p \pm Te'_p \quad (4)$$

Where  $M_{p,p}$  and  $M'_{p,p}$  are simplified plastic moment resistances of a prestressed composite section in positive and negative bending respectively;  $M_p$  and  $M'_p$  are plastic moment resistances of a non-prestressed section;  $T$  is prestressing force, and  $e_p$  and  $e'_p$  are eccentricity of the tendon force to the centroid of composite cross-section in positive and negative bending respectively.

As discussed previously, the incremental stress of the tendons would develop at the ultimate limit state of the beam and frictions at the intermediate draped points also caused the differences of prestressing forces at the different segments of the tendons. The measured mean prestressing forces were 121.6 kN at the initial stage and 164.4 kN at the ultimate failure. The mean incremental prestressing force at the ultimate state is 35% of the initial prestressing force, and it should have the secondary bending action on the beam. The moment resistances of beams CCB1 and PCCB1 at different stages are given in Table 4, in which the initial prestressing forces are used in calculation of  $M_{p,p}$  and  $M'_{p,p}$  for the prestressed beam. If the measured ultimate prestressing forces are used, the corresponding positive and negative plastic moments are 370.1 kNm and 270.9 kNm respectively. For simplicity but on the safe side, initial prestressing force  $T_{ini}$  could be used in Eqs. (3) and (4). In the following discussions, the same notations of moment resistances are used for both CCB1 and PCCB1.

As illustrated in Table 4, the predicted cracking moments are slight higher than the test results. Considering the moment contributed from self weight of the beams which was not measured in the tests, being 3.4 kNm in the internal support section, the predicted values agree well with the test results.

It should be noticed that the measured moments  $M'_y$  defined as yielding occurrence in the internal support section are much lower than calculated yield moment resistances in negative bending for the both beams. Even the maximum moments  $M_{h,max}$  (207.7 kNm for CCB1 and 208.0 kNm for PCCB1) at the internal supports in the tests are slightly lower than their calculated yield moment resistances as listed in Table 4. The maximum measured mid-span moments however, are much greater than the calculated plastic moment resistances in positive bending. The main reasons for this phenomenon are owing to the buckling either distortional or local, which initiated in hogging moment regions of the beams earlier before yielding, and governed the capable moment of the cross-sections in negative bending. Since beams (CCB1 and PCCB1) are classified as class 3 section, the maximum moment capable in negative bending is the yielding moment. Restrained to the maximum capable moment at the internal support section, when the load continuously increased, moment redistributed from the internal support to the mid-span regions in the beams, and full plasticity and even extra plasticity are expected to develop in the mid-spans.

Analysis of test results shows that adding prestressing with external tendons can increase the cracked moment resistance of a composite beam, but not the yield moment resistance in negative bending. Distortional lateral buckle and local buckle or interactive mode of the two should govern the ultimate hogging moment capable in a prestressed continuous composite beam.

Table 4 Calculated moment resistances of beams CCB1 and PCCB1

Specimens	In positive moment		In negative moment		
	$M_y$ : kNm	$M_p$ : kNm	$M_{crack}$ : kNm	$M'_y$ : kNm	$M'_p$ : kNm
CCB1	254.1	293.1(344.2)	19.7(16.7)	217.4(174.5)	263.3
	$M_{y,p}$ : kNm	$M_{p,p}$ : kNm	$M_{crack,p}$ : kNm	$M_{y,p}'$ : kNm	$M_{p,p}'$ : kNm
PCCB1	294.1	349.3(407.7)	49.2(43.8)	230.7(167.9)	268.5

Notes: the figures with ( ) are test results.

### 3.3 Evaluation of moment redistribution

Moment redistribution based on a global elastic analysis is now widely accepted as a practical design method for the ultimate limit state of continuous composite beams. The analysis can be based either on uncracked sections or cracked sections, and it is essential to estimate moment redistribution capable of in assessment of the load carrying capacity of an external prestressed continuous composite beam.

As being discussed, substantial moment redistributed from the hogging region to the sagging region was observed in both the non-prestressed and the prestressed composite continuous beams. In design practice, moment redistribution is defined based on a global elastic analysis for non-prestressed continuous beams only. What influence the prestressing force possessing of on the moment redistribution in prestressed composite beams however, has not been addressed in public references. By definition, moment redistribution ratio is defined as the follows

$$\beta = \frac{M_e - M_u}{M_e} \tag{5}$$

Where  $\beta$  is moment redistribution ratio,  $M_e$  is the calculate moment derived from a global elastic analysis at the ultimate load, and  $M_u$  is the plastic moment resistance. Based on the test results, moment redistribution developed in beams CCB1 and PCCB1 is evaluated. In Table 5, the predict elastic moment is calculated from a global elastic analysis with uniform uncracked section and the moment redistributions developed at the internal support section and at the mid-span section for the tested beams are listed.

In continuous composite beams, restrained by either local or distortional buckling, the extent of nonlinear plasticity to develop is rather complicated due to the sagging moment capacity of the cross-section normally being significantly larger than the hogging moment capacity. As illustrated in Table 5, the maximum moments at the internal support attained in the tests are all lower than the calculated yield moment resistances for both beams. At the ultimate state, moment redistribution in hogging regions of the two beams is more than 40%. In terms of the maximum moment attainable, it is not logic and worth of argument why the plastic moment resistance not the true ultimate moment such as  $M'_{u, test}$  is used in assessment of the moment redistribution. Moreover, it appears more available moment redistribution in the beams if the true values  $M'_{u, test}$  are adopted accordingly as expressed in Eq. (5), which is inconsistent to the fact that moment redistribution would be affected and reduced by the buckling feature.

Based on equilibrium of the test specimens (right beam segment shown in Fig. 2) at the ultimate failure state, the load carrying capacity of the beams  $P$  can be written as

Table 5 Moment redistribution in sagging and hogging regions (CCB1, PCCB1)

Specimen	$P_{max}$ kN	T kN	At internal support section				At mid-span section			
			$M'_p$ kNm	$M'_{u, test}$ kNm	$M'_c$ kNm	$\beta_{hog}$	$M_p$ kNm	$M_{u, test}$ kNm	$M'_c$ kNm	$\beta_{sag}$
CCB1	557.2	0	263.3	207.7	445.8	0.41	254.1	344.2	223.0	-0.14
PPCB1	618.5	242	268.5	208.0	494.8	0.46	294.1	407.7	247.4	-0.19

$$P = 3 \left( 2 \frac{M_{s,u}}{L} + \frac{M_{h,u}}{L} \right) \quad (6)$$

where  $M_{s,u}$  and  $M_{h,u}$  are the maximum moment at the mid-span and at the internal support sections respectively, and  $L$  is the beam span. Being restrained by local or distortional buckling, the capable moment at the internal support section is the yield moment for class 3 cross-section. Replace  $M_{s,u}$  with  $M_p$  and  $M_{h,u}$  with  $M_y'$  (given in Table 4) for both specimens CCB1 and PCCB1, the calculated load carrying capacity  $P$  is 502.3kN ( $0.9 P_{\max,\text{test}}$ ) for CCB1 and is 580.8 kN ( $0.94 P_{\max,\text{test}}$ ) for PCCB1.

Another approach is to evaluate moment redistribution in mid-span regions of the beams which should be more rational. Being restricted to distortional or local buckling, substantial loading was shed to the mid-span region from the hogging moment region. In terms of moment redistribution in sagging moment region, then the calculated design moment  $M_e$  is expressed as

$$M_e = (1 - \beta)M_p \quad (7)$$

where  $M_p$  is the plastic moment resistance of cross-section, and can be calculated by Eq. (3). The moment redistribution ratio  $\beta$  is  $-0.14$  and  $-0.19$  for CCB1 and PCCB1 respectively in the present study.

#### 4. Conclusions

Two continuous composite beams were investigated experimentally. One of the beams was a conventional composite continuous beam, while the other was a prestressed composite continuous beam. Test investigation demonstrated that being prestressed with external tendons, the cracked moment resistance of a composite beam can be increased effectively, however the yield moment in negative bending of the beam will not always, as being expected, increase.

For both the prestressed and the non-prestressed continuous beams, lateral, distortional and local buckling initiated in web and in compression flanges. Full plasticity was developed in the mid-span section even when lateral or distortional buckling initiated in the hogging moment regions for both beams. The prestressed beam sustained a higher sagging moment than that of the non-prestressed beam in the mid-span. More moment appears to redistribute from the hogging region to the mid-span regions in the prestressed beam than that in the non-prestressed beam.

#### Acknowledgements

This research was made possible through the financial supports of the National Science Foundation of China (50678132). The funding, cooperation and assistance of many people from the organization are greatly acknowledged. The author also acknowledges with thanks the provision of steel work by Huaying Steel Work Company, and the assistance of the technicians at the State Laboratory of Disaster Reduction in Civil Engineering of Tongji University.

## References

- Ayyub, B.M., Sohn, Y.G. and Saadatmanesh, H. (1990), "Prestressed composite girders under positive moment", *J. Struct. Eng.*, **116**(11), 2931-2951.
- Ayyub, B.M., Sohn, Y.G. and Saadatmanesh, H. (1992), "Prestressed composite girders I: Experimental study for negative moment", *J. Struct. Eng.*, **118**(10), 2743-2762.
- Ayyub, B.M., Sohn, Y.G. and Saadatmanesh, H. (1992), "Prestressed composite girders II: Analytical study for negative moment", *J. Struct. Eng.*, **118**(10), 2763-2783.
- Chen, S. (2005), "Experimental study of prestressed steel-concrete composite beams with external tendons for negative moment", *J. Constr. Steel Res.*, **61**(12), 1613-1630.
- Chen, S. (2006), "Discussion of Finite element model for externally prestressed composite beams with deformable connection", *J. Struct. Eng.*, **132**(12), 2036-2038.
- Chen, S. and Gu, P. (2005), "Load carrying capacity of composite beams prestressed with external tendons under positive moment", *J. Constr. Steel Res.*, **61**(4), 515-530.
- Chen, S. and Zhang, Z. (2006), "Effective width of a concrete slab in steel-concrete composite beams prestressed with external tendons", *J. Constr. Steel Res.*, **62**(5), 493-500.
- Dall'Asta, A. and Zona, A. (2005), "Finite element model for externally prestressed composite beams with deformable connection", *J. Struct. Eng.*, **131**(5), 706-714.
- European Committee for Standardisation. Eurocode 4 *Design of composite steel and concrete structures*. Part 1.1: General rules and rules for buildings, CEN, Brussels, ENV1994-1-1.
- Lorenc, W. and Kubica, E. (2006), "Behavior of composite beams prestressed with external tendons: Experimental study", *J. Constr. Steel Res.*, **62**(12), 1353-1366.
- Nie, J.G., Cai, C.S., Zhou, T.R. and Li, Y. (2007), "Experimental and analytical study of prestressed steel-concrete composite beams considering slip effect", *J. Struct. Eng.*, **133**(4), 530-540.
- Saadatmanesh, H., Albrecht, P. and Ayyub, B.M. (1989), "Experimental study of prestressed composite beams", *J. Struct. Eng.*, **115**(9), 2348-2363.
- Uy, B. and Craine, S. (2004), "Static flexural behavior of externally post-tensioned steel-concrete composite beams", *Adv. Struct. Eng.*, **7**(1), 1-20.
- Xue, W., Ding, M., He, C. and Li, J. (2008), "Long-term behavior of prestressed composite beams at service loads for one year", *J. Struct. Eng.*, **134**(6), 930-937.
- Zona, A., Ragni, L. and Dall'Asta, A. (2009), "Simplified method for the analysis of externally prestressed steel-concrete composite beams", *J. Constr. Steel Res.*, **65**(2), 308-313.
- Zong, Z. *et al.* (2002), "Experimental study of external prestressed steel-concrete composite continuous beams", *China J. Highway Transport*, **15**(1), 44-49.